RESEARCH ARTICLE

Figures and figure supplements

Maternally inherited piRNAs direct transient heterochromatin formation at active transposons during early *Drosophila* embryogenesis

Martin H Fabry *et al*

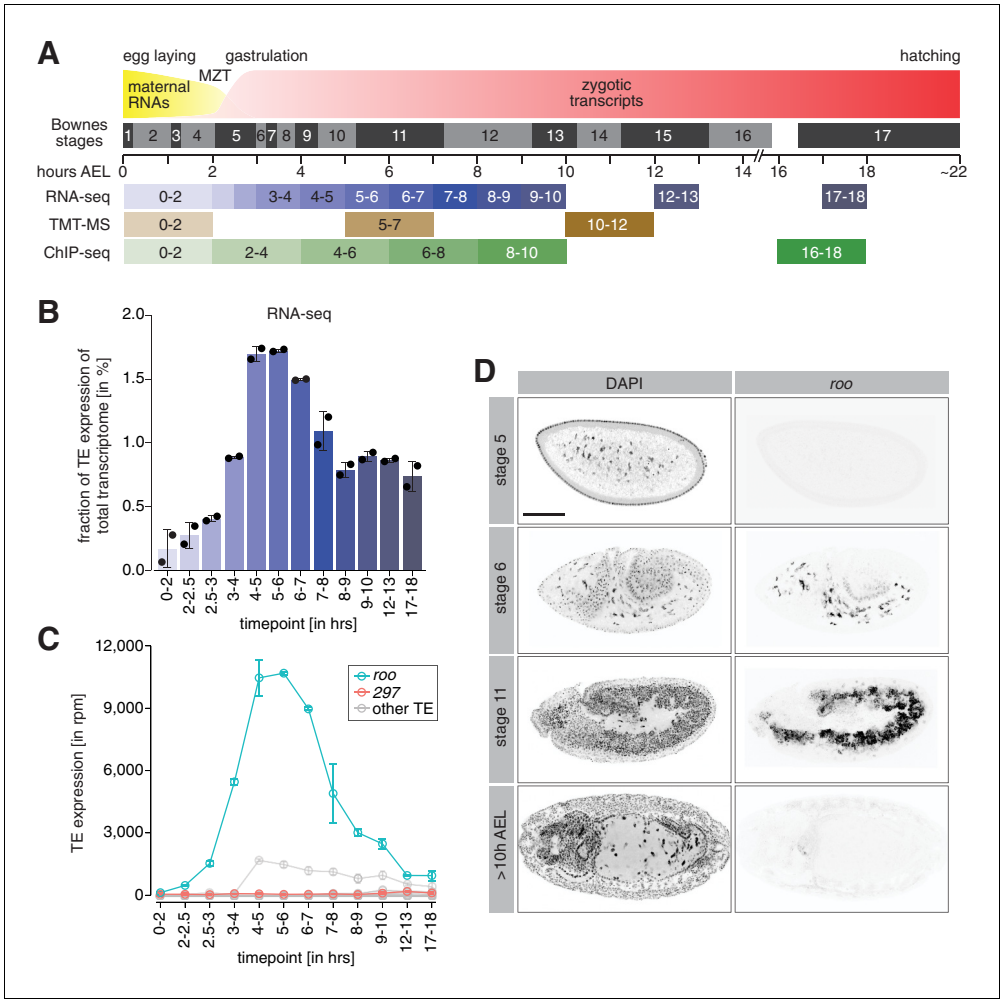

Figure 1. A transient burst of transposon expression during *Drosophila* embryogenesis. (**A**) Schematic of *Drosophila* embryogenesis indicating Bownes stages and collected time points. (**B**) Bar graphs showing contribution of transposon derived reads to the transcriptome of control w^{1118} embryos at the indicated time points in percent. Error bars show standard deviation (n = 2). (**C**) Line graphs showing the RNA expression (in rpm) for the 30 most expressed transposons during the indicated time points of embryogenesis. Error bars show standard deviation (n = 2). (**D**) Confocal fluorescent microscopy images of control w^{1118} embryos showing nuclei stained with DAPI and *roo* transcripts by RNA-FISH at the indicated embryonic stages (also see ***Figure 1—figure supplement 2B***). Scale bar = 100 μm.

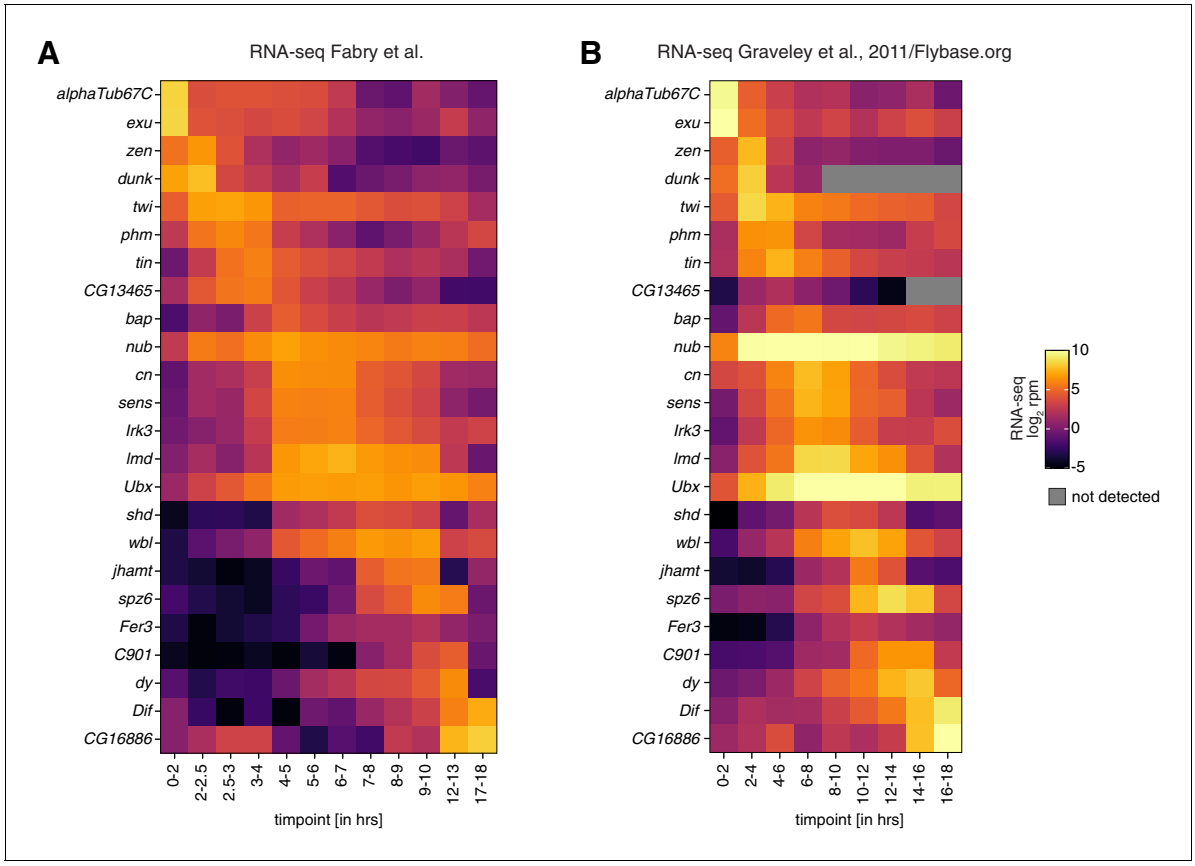

Figure 1—figure supplement 1. Correlation of embryo collection time points between datasets. (**A**) Heatmaps showing expression changes in RNA-seq (in $\log_2$ reads per million; n = 2) of control w^{1118} embryos for the indicated time points and selected genes with dynamic expression during embryogenesis. (**B**) As in (**A**) but showing reanalyzed datasets published by Graveley and colleagues (***Graveley et al., 2011***). Gray squares = not detected.

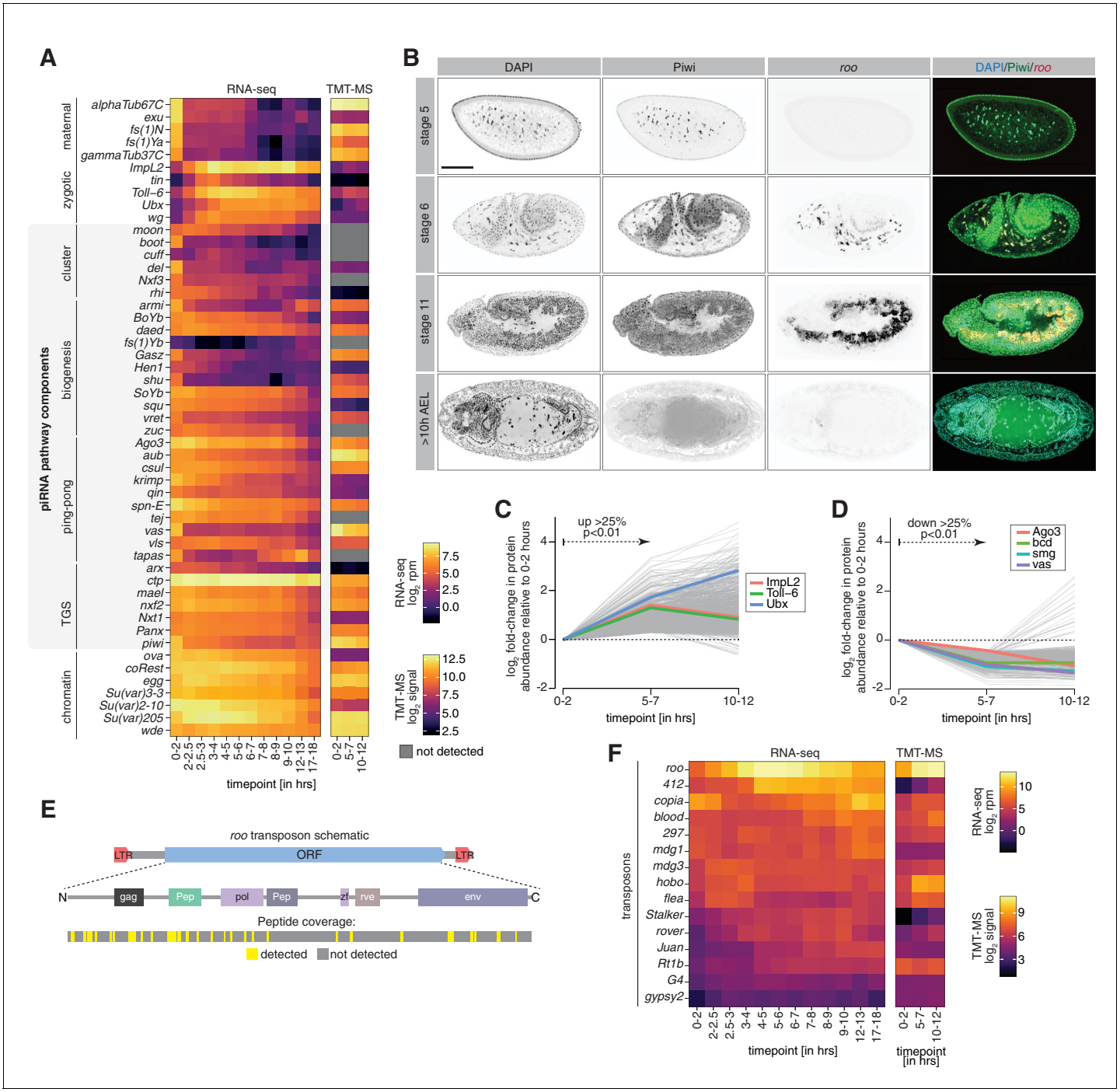

Figure 1—figure supplement 2. Transposon protein and the known cohort of piRNA co-transcriptional gene silencing (coTGS) factors are present during embryogenesis. (**A**) Heatmaps showing expression changes in RNA-seq (left; in log_2 reads per million; n = 2) and protein abundance in TMT-MS (right; log_2 signal intensity; n = 3) of control w^{1118} embryos for indicated time points and selected maternal/zygotic genes, chromatin factors, and the indicated piRNA pathway components. Gray squares = not detected. (**B**) Confocal fluorescent microscopy images of embryos showing immunofluorescence staining for Piwi protein, *roo* transcripts by RNA-FISH and nuclei with DAPI at the indicated embryonic stages. Scale bar = 100 µm. (**C**) Line graphs showing fold-changes in protein abundance (relative to 0–2 hr after egg laying [AEL]) measured by quantitative mass spectrometry for indicated time points of control w^{1118} embryos. Shown are genes with increasing protein abundance (over 25% with p<0.01) between 0–2 hr and 5–7 hr AEL. (**D**) As in (**C**) but showing genes with protein abundance decreasing (over 25% with p<0.01). (**E**) Schematic indicating the LTR-flanked 272 kDa open reading frame (ORF) of *roo* and its coding potential. Gag: group-specific antigen-like protein; pol: reverse transcriptase; env: envelope protein; Pep: two peptidases; zf: zinc finger-associated domain. Peptides detected by TMT-MS are indicated in yellow, regions not detected are shown in gray. (**F**) Heatmap showing protein signal intensity (arbitrary units) of the indicated transposons and time points in control w^{1118} embryos (n = 3).

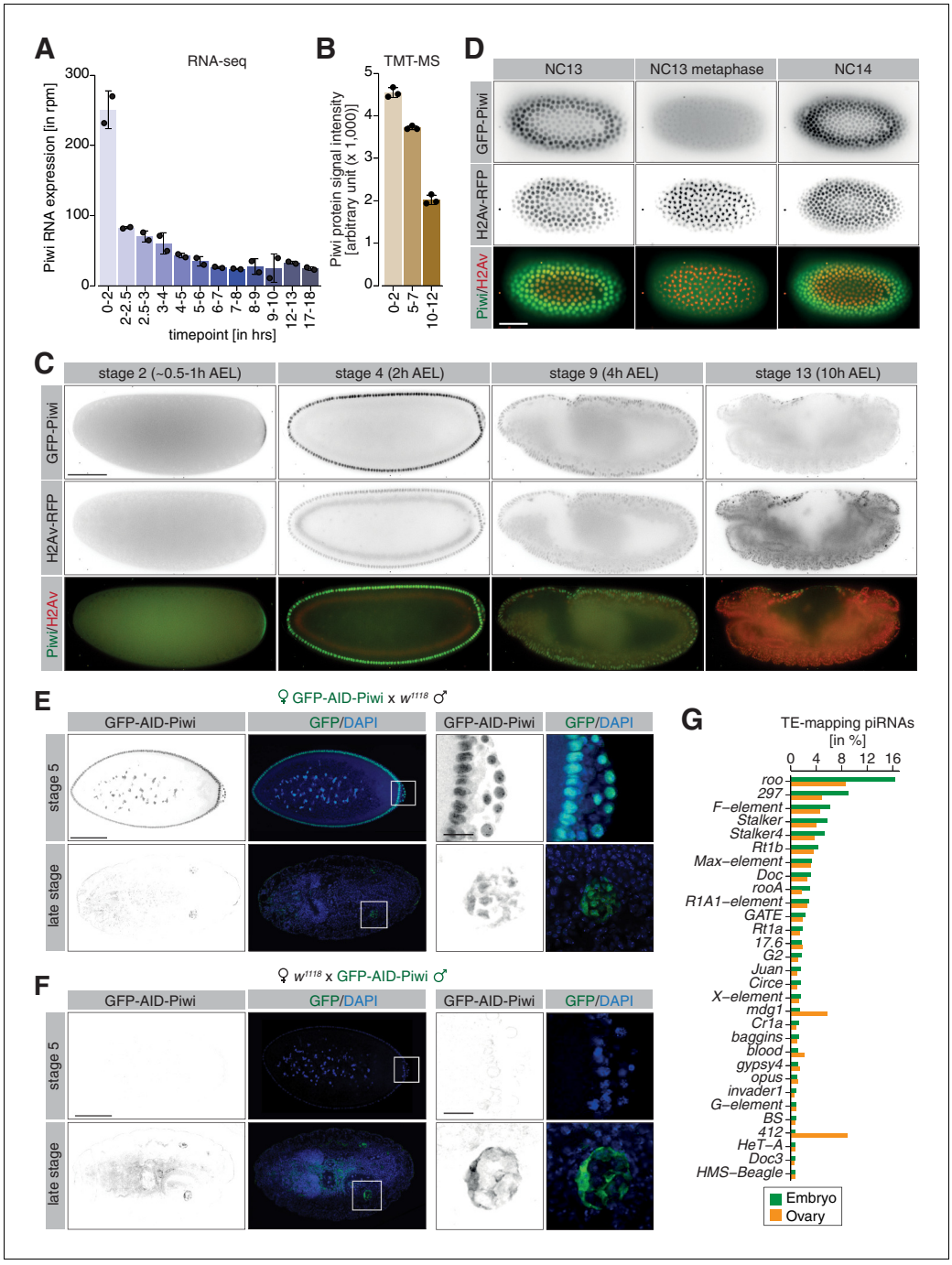

Figure 2. piRNA co-transcriptional gene silencing (coTGS) factors are maternally inherited and localize to somatic cells of the *Drosophila* embryo. (**A**) Bar graphs showing Piwi RNA expression (in rpm) at the indicated time points in control w^{1118} embryos. Error bars show standard deviation (n = 2). (**B**) Bar graphs showing Piwi protein signal intensity (arbitrary units) at the indicated time points in control w^{1118} embryos. Error bars show standard deviation (n = 3). (**C**) Stand-still images from ***Video 1*** obtained by light-sheet fluorescent live microscopy of embryos derived from parents expressing GFP-Piwi (green) and H2Av-RFP (red) for the indicated time points. Scale bar = 50 µm. (**D**) As in (**C**) but showing the transition from NC13 to NC14. Scale bar = 50 µm. (**E**) Confocal fluorescent microscopy images of embryos derived from females expressing GFP-AID-Piwi crossed to control w^{1118} males probing for GFP and DAPI. Shown are embryos at the blastoderm stage (stage 5) and late-stage embryos (>12 hr after egg laying). Scale bar = 100 µm. Zoom of the indicated regions showing developing germ cells. Scale bar = 10µm. (**F**) As in (**E**) but showing embryos derived from control w^{1118} females crossed to GFP-AID-Piwi males. (**G**) Bar graph showing small RNA-seq from Piwi immunoprecipitation of 0–8 hr control w^{1118} embryos (green, n = 1) or adult ovaries

Figure 2 continued on next page

Figure 2 continued

(orange, n = 1). Shown are antisense piRNAs of the 30 most abundant TE families in embryos as percentage of reads mapping to indicated transposons relative to all transposable element-mapping antisense piRNAs.

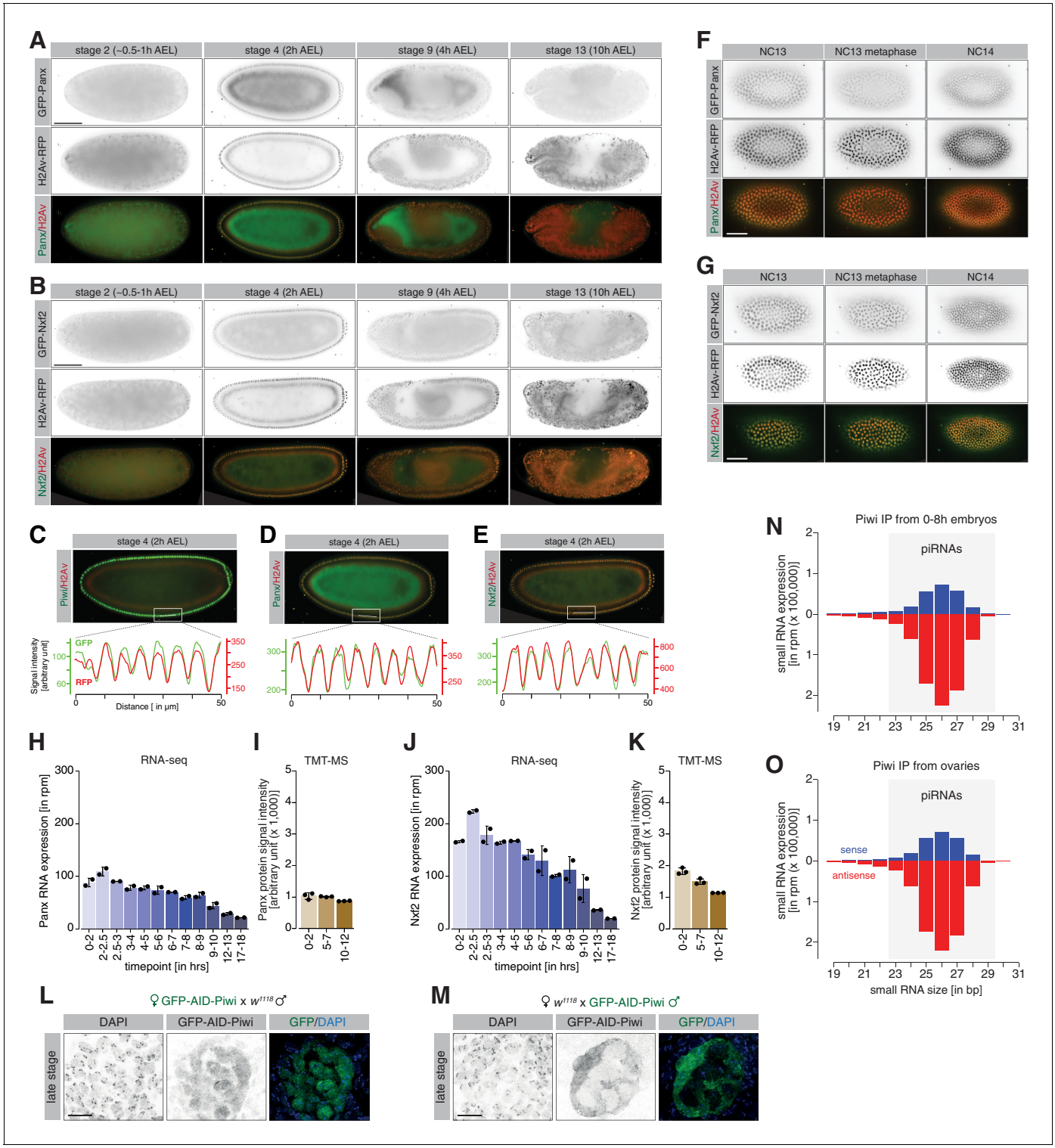

Figure 2—figure supplement 1. Maternally inherited co-transcriptional gene silencing (coTGS) factors localize to nuclei of pole and somatic cells during embryogenesis. (**A**) Stand-still images from ***Video 2*** obtained by light-sheet fluorescent live microscopy of embryos derived from parents expressing GFP-Panx (green) and H2Av-RFP (red) for the indicated time points. Scale bar = 50 µm. (**B**) As in (**A**) but showing stand-still images from ***Video 3*** for GFP-Nxf2 (green) and H2Av-RFP (red) for the indicated time points. Scale bar = 50 µm. (**C**) Quantification of co-localization between GFP-Piwi and H2Av-RFP. Plot profile shows relative intensity of GFP-Piwi (green) and H2Av-RFP (red) protein for the indicated section (white line) of stage 4 (2 hr after egg laying) embryos. (**D**) As in (**C**) but showing embryos expressing GFP-Panx and H2Av-RFP. (**E**) As in (**C**) but showing embryos expressing GFP-Nxf2 and H2Av-RFP. (**F**) As in (**A**) but showing the transition of GFP-Panx from NC13 to NC14. Scale bar = 50 µm. (**G**) As in (**B**) but showing the

Figure 2—figure supplement 1 continued on next page

Figure 2—figure supplement 1 continued

transition of GFP-Nxf2 from NC13 to NC14. Scale bar = 50 μm. (**H**) Bar graphs showing Panx RNA expression (in rpm) at the indicated time points in control w^{1118} embryos. Error bars show standard deviation (n = 2). (**I**) Bar graphs showing Panx protein signal intensity (arbitrary units) at the indicated time points in control w^{1118} embryos. Error bars show standard deviation (n = 3). (**J**) As in (**H**) but showing the Nxf2 RNA expression. (**K**) As in (**I**) but showing Nxf2 protein expression. (**L**) Confocal fluorescent microscopy images of developing germ cells of late-stage embryos derived from females expressing GFP-AID-Piwi crossed to control w^{1118} males probing for GFP and DAPI. Scale bar = 10 μm. (**M**) As in (**L**) but showing developing germ cells of late-stage embryos derived from control w^{1118} females crossed to GFP-AID-Piwi males. (**N**) Bar graph showing size distribution of Piwi-associated small RNAs (in rpm) from 0 to 8 hr w^{1118} embryos (n = 1). Blue = sense, red = antisense. (**O**) As in (**N**) but showing Piwi-associated small RNAs from adult w^{1118} ovaries (n = 1).

Figure 3. Transposon insertions targeted by piRNAs in embryos show epigenetic changes characteristic of co-transcriptional gene silencing. (**A**) Heatmaps (top) and metaplots (bottom) showing H3K9me3 ChIP-seq signal (in rpm) for the indicated embryonic stages and adult tissues at 117 euchromatic, w^{1118}-specific *roo* insertions (n = 2). Signal is shown within 10 kb from insertion site and sorted from 5′ to 3′. (**B**) UCSC genome browser screenshot showing H3K9me3 ChIP-seq signal for the indicated genes on chromosome 2R carrying w^{1118}-specific *roo* and *Doc* insertions.

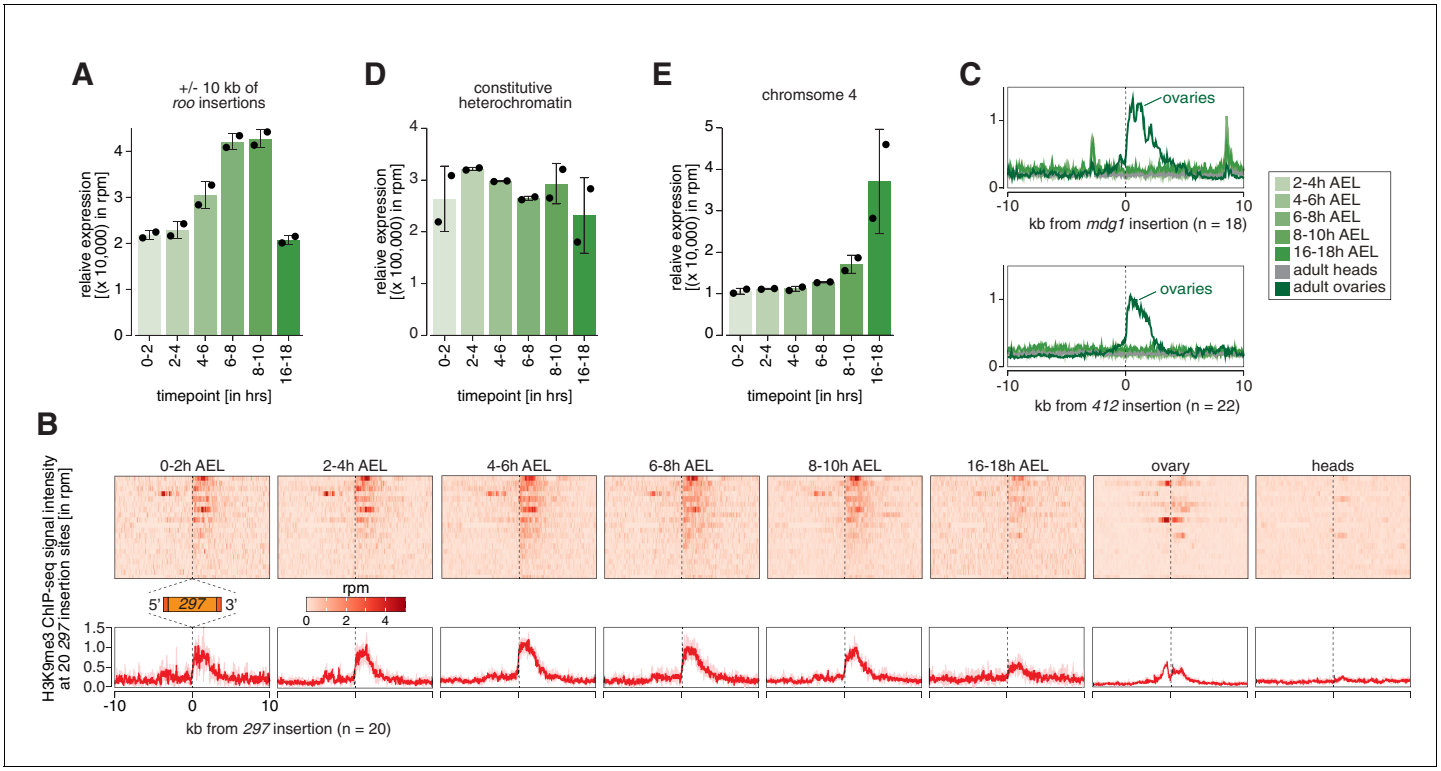

Figure 3—figure supplement 1. Transposons targeted by maternally inherited piRNAs show hallmarks of co-transcriptional gene silencing (coTGS). (**A**) Bar graphs showing H3K9me3 signal intensity for the indicated time points at *roo* insertions. Error bars show standard deviation (n = 2). (**B**) Heatmaps (top) and metaplots (bottom) showing H3K9me3 ChIP-seq signal (in rpm) for the indicated embryonic stages and adult tissues at 20 euchromatic, w^{1118}-specific *297* insertions (n = 2). Signal is shown within 10 kb from insertion site and sorted from 5′ to 3′. (**C**) Metaplots showing H3K9me3 ChIP-seq signal (in rpm) for the indicated embryonic stages and adult tissues at 18 euchromatic, w^{1118}-specific *mdg1* (top) and at 22 euchromatic, w^{1118}-specific *412* insertions. Signal is shown within 10 kb from insertion site and sorted from 5′ to 3′ (n = 2). (**D**) Bar graphs showing H3K9me3 signal intensity for the indicated time points at constitutive heterochromatin. Error bars show standard deviation (n = 2). (**E**) As in (**D**) but showing chromosome 4 regions.

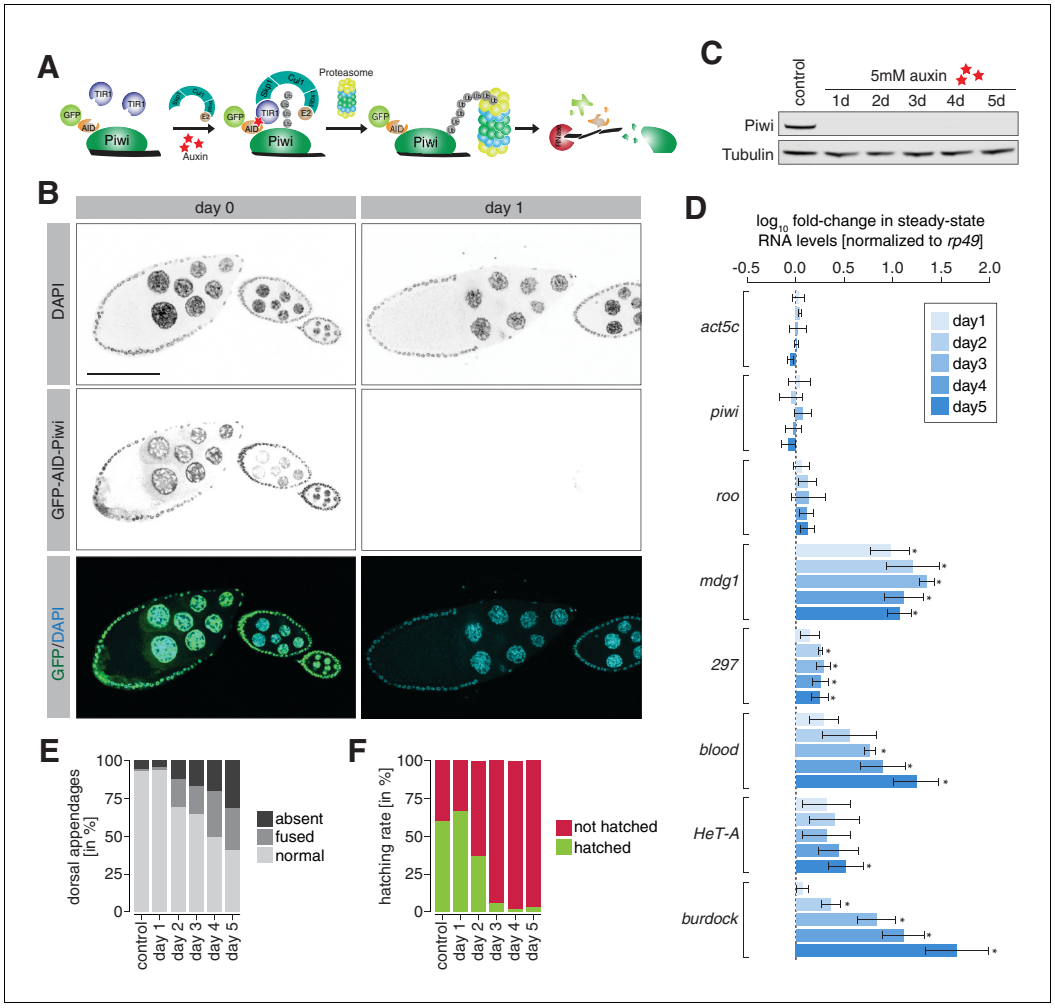

Figure 4. Degradation of Piwi protein in ovaries resembles mutant phenotypes. (**A**) Cartoon illustrating the Piwi protein degradation strategy using the auxin-inducible AID-TIR1 system. (**B**) Confocal fluorescent microscopy images showing ovary egg chambers of GFP-AID-Piwi; OsTIR1 flies fed with yeast paste containing 5 mM auxin for the indicated time (also see ***Figure 4—figure supplement 1A***). Blue = DAPI. Green = GFP-AID-Piwi. (**C**) Western blot of ovaries from females treated with 5 mM auxin-containing yeast paste for the indicated time period or control females probing for Piwi and Tubulin as a loading control. (**D**) Bar graphs showing *rp49*-normalized steady-state RNA levels of the indicated transposable elements and control genes in ovaries of GFP-AID-Piwi; OsTIR1 flies fed with yeast paste containing 5 mM auxin for the indicated time. Error bars show standard deviation (n = 3). Asterisk denotes significant changes compared to control ($p<0.05$, unpaired t-test). (**E**) Bar graphs showing the percentage of embryo deformation phenotypes laid by GFP-AID-Piwi; OsTIR1 females fed with yeast paste containing 5 mM auxin for the indicated time. (**F**) As in (**E**) but showing the hatching rate in percent.

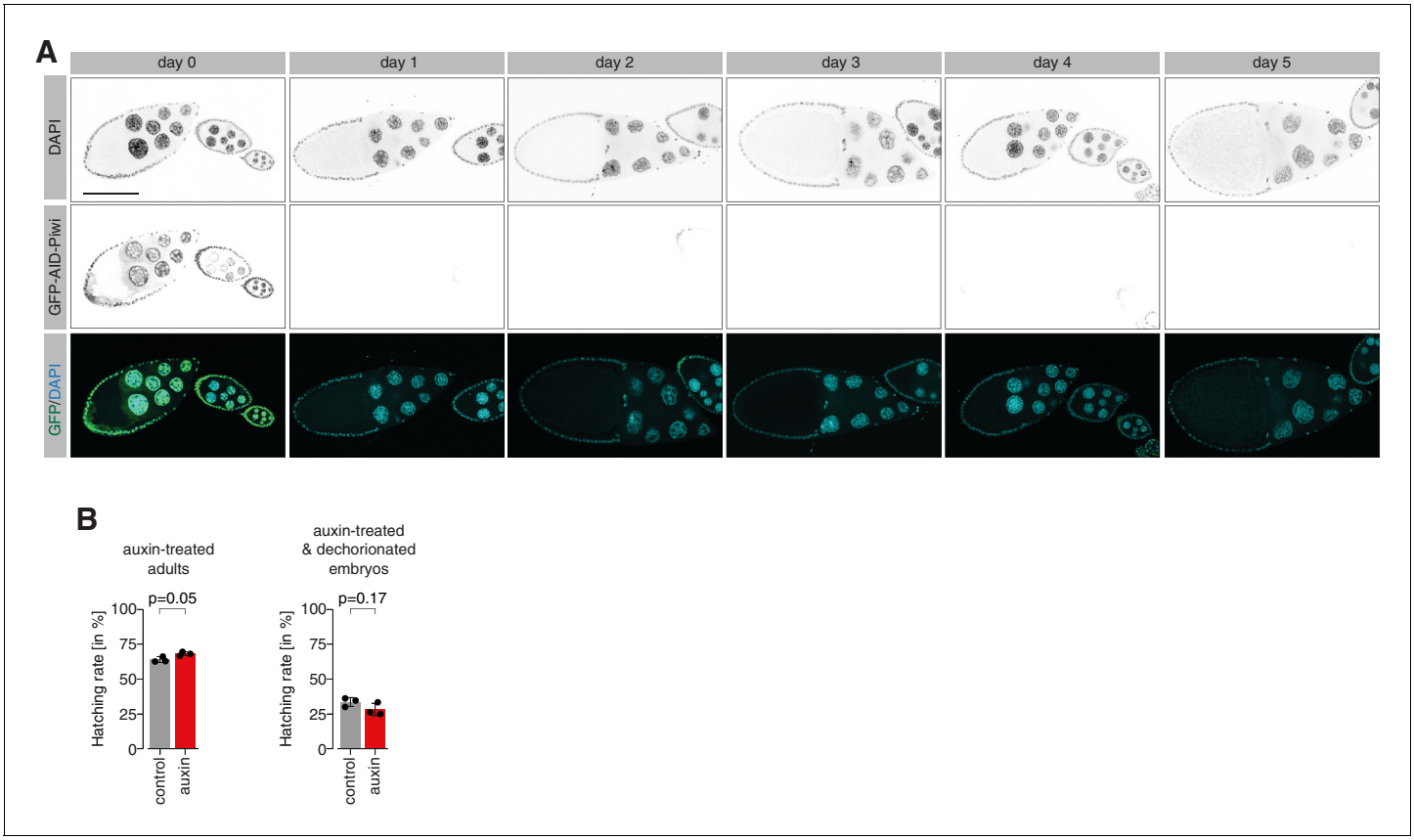

Figure 4—figure supplement 1. Piwi degradation in ovaries resembles knockdown and mutant phenotypes. (**A**) Confocal fluorescent microscopy images showing ovary egg chambers of GFP-AID-Piwi; OsTIR1 flies fed with yeast paste containing 5 mM auxin for the indicated time. Blue = DAPI, green = GFP-AID-Piwi. (**B**) Bar graphs showing the percentage of hatched embryos laid by auxin- or control-treated females after 24 hr (left) and of embryos treated for 2.5 hr with 5 mM auxin following dechorionation (right). Statistical significance was determined by unpaired (two-sample) t-test.

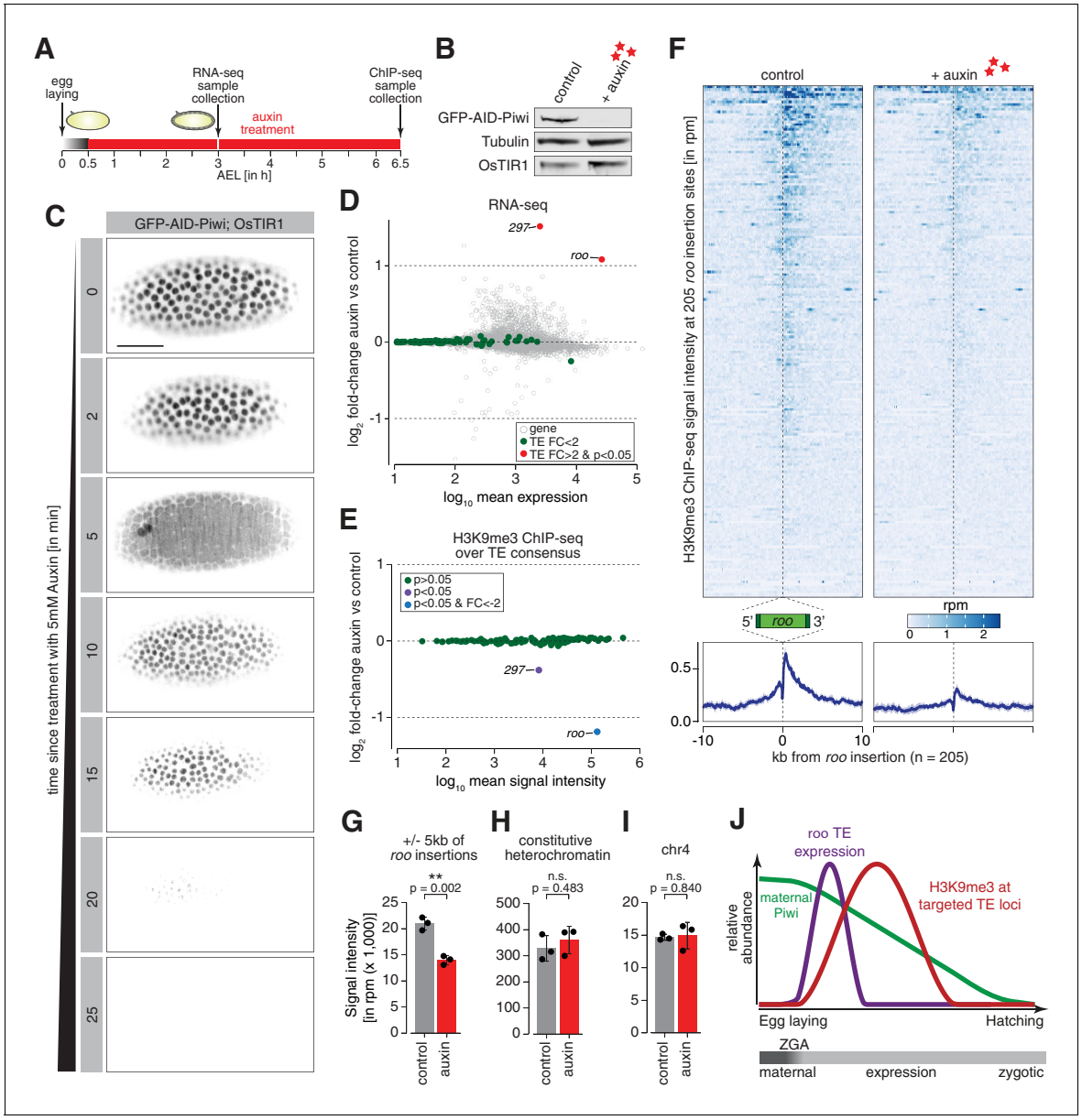

Figure 5. Degradation of maternally deposited Piwi in embryos leads to transposon deregulation. (**A**) Schematic of embryo auxin treatments and sample collection for RNA-seq and ChIP-seq experiments. (**B**) Western blot showing abundance of GFP-AID-Piwi fusion protein in embryos treated with 5 mM auxin for 2 hr. OsTIR1 and tubulin expression are shown as loading control. (**C**) Stand-still images from ***Video 4*** obtained by light-sheet fluorescent live microscopy of embryos derived from parents expressing GFP-AID-Piwi and OsTIR1 treated with 5 mM auxin for the indicated time intervals. Scale bar = 50 µm. (**D**) MA plot showing base mean expression (log_{10} scale) of transposon RNAs relative to their fold-change (log_2 scale) in GFP-AID-Piwi; OsTIR1 embryos treated with 5 mM auxin versus control (n = 3). Gray = genes, green = TEs not changed (p<0.05), red = transposable elements (TEs) significantly changed (p<0.05) and fold-change > 2. (**E**) MA plot showing base mean signal intensity (log_{10} scale) of TEs relative to the H3K9me3 ChIP-seq signal enrichment (log_2 scale) in GFP-AID-Piwi; OsTIR1 embryos treated with 5 mM auxin versus control (n = 3). Gray = TEs not significantly changed (p>0.05), purple = TEs significantly changed (p<0.05), blue = TEs significantly changed (p<0.05) and fold-change < –2. (**F**) Heatmaps (top) and metaplots (bottom) showing H3K9me3 ChIP-seq signal (in rpm) for control embryos and 5 mM auxin-treated embryos at 205 euchromatic, degron strain-specific *roo* insertions (n = 3). Signal is shown within 10 kb from insertion site and sorted from 5′ to 3′. (**G**) Bar graphs showing H3K9me3 signal intensity (in rpm) for the indicated treatments at *roo* loci. Error bars show standard deviation (n = 3). Statistics were calculated with unpaired (two-sample) t-test. (**H**) As in (**G**) but showing constitutive heterochromatin. (**I**) As in (**G**) but showing chromosome 4 regions. (**J**) Model of piRNA-guided chromatin modification at active transposons in somatic cells of the developing *Drosophila* embryo.

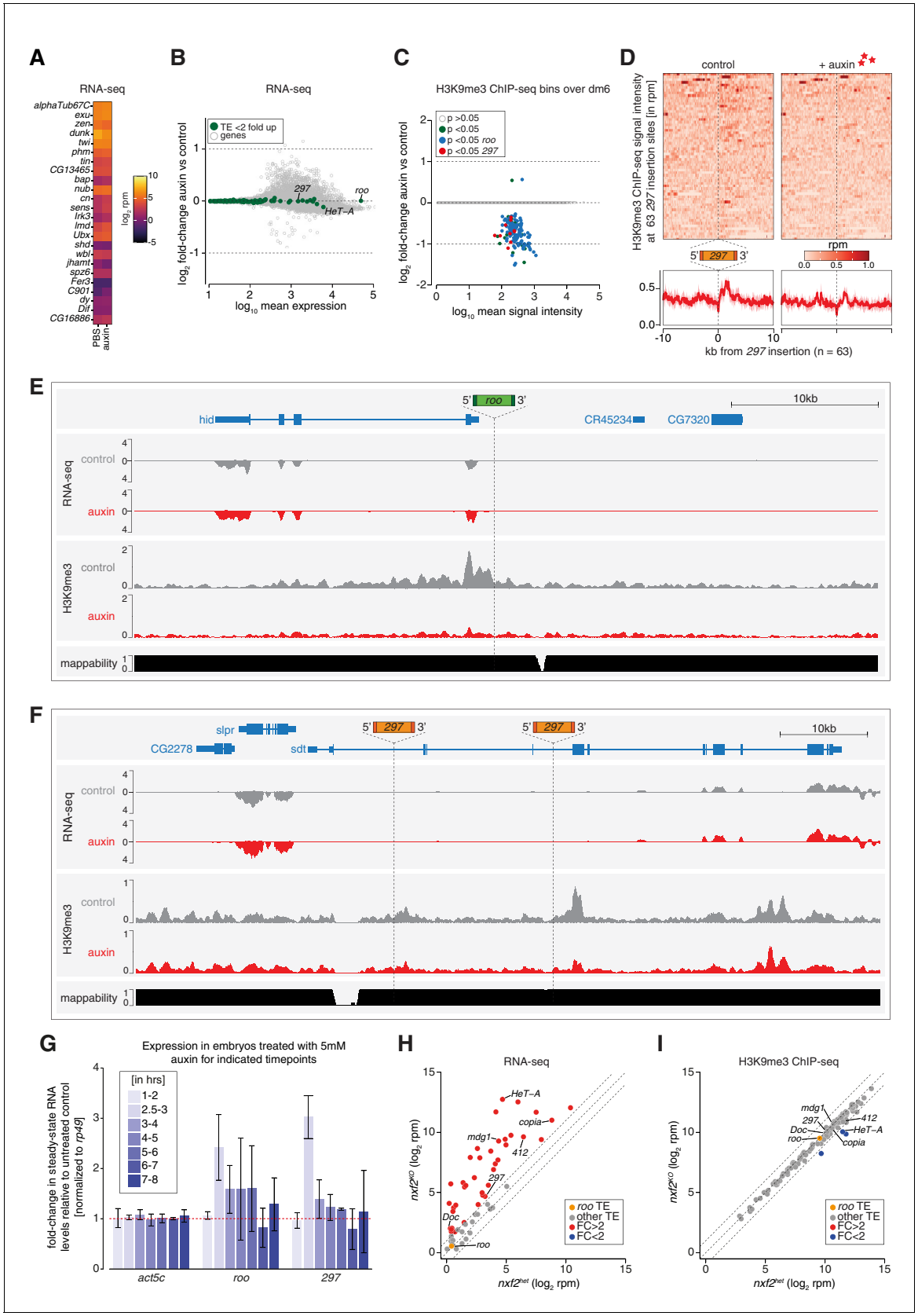

Figure 5—figure supplement 1. Piwi depletion in embryos leads to epigenetic changes at transposable element (TE) insertions targeted by maternally inherited piRNAs. (**A**) Heatmap comparing expression profiles of selected genes (same as shown in ***Figure 1—figure supplement 1***) in RNA-seq (in

Figure 5—figure supplement 1 continued on next page

Figure 5—figure supplement 1 continued

log_2 reads per million) of 2.5–3 hr PBS or auxin-treated embryos of genotype GFP-AID-Piwi; OsTIR1 (n = 3). (**B**) MA plot showing base mean expression (log_{10} scale) of genes and transposons relative to their fold-change (log_2 scale) in GFP-AID-Piwi embryos (without OsTIR1) treated with 5 mM auxin versus control (n = 3). Gray = genes, green = TEs not changed (p>0.05). (**C**) MA plot showing base mean signal intensity (log_{10} scale) of TEs relative to the H3K9me3 ChIP-seq signal within 5 kb genomic bins of GFP-AID-Piwi; OsTIR1 embryos treated with 5 mM auxin versus control (n = 3). Gray = unchanged (p>0.05), green = significantly changed (p<0.05), blue = significantly changed (p<0.05) within 5 kb of a *roo* insertion, red = significantly changed (p<0.05) within 5 kb of a *297* insertion. (**D**) Heatmaps (top) and metaplots (bottom) showing H3K9me3 ChIP-seq signal (in rpm) for control embryos and 5 mM auxin-treated embryos at 63 euchromatic, degron strain-specific *297* insertions (n = 3). Signal is shown within 10 kb from insertion site and sorted from 5′ to 3′. (**E**) UCSC genome browser screenshot showing RNA-seq and H3K9me3 ChIP-seq signal of control and auxin-treated embryos (derived from flies homozygous for GFP-AID-Piwi; OsTIR1) at the indicated, degron strain-specific *roo* insertion on chromosome 3L. (**F**) As in (**E**) but showing a genomic locus with two degron strain-specific *297* insertion sites. (**G**) Bar graphs showing *rp49*-normalized steady-state RNA levels of the indicated TEs and control gene in GFP-AID-Piwi; OsTIR1 embryos at the indicated time intervals (after egg laying [AEL]) treated with 5 mM auxin compared to PBS-treated control embryos. Error bars show standard deviation (n = 2). (**H**) Scatter plot showing RNA expression levels (in rpm, log_2 scale) of transposons from ovaries of *nxf2* heterozygote and homozygote mutants (n = 3). Transposons whose abundance change more than twofold compared to heterozygotes are highlighted in red, *roo* is shown in orange. Data reanalyzed from ***Fabry et al., 2019***. (**I**) As in (**H**) but showing H3K9me3 ChIP-seq levels. Transposons with more than twofold reduced levels in the mutant compared to heterozygotes are shown in blue.